A Dynamical Model for the Transmembrane Potential Regulation by pH

Araks Martirosyan, Loïc Paulevé, Clair Poignard, Mireille Régnier, Jean-Marc Steyaert, Laurent Schwartz

A Dynamical Model for the Transmembrane Potential Regulation by pH

Araks Martirosyan[1,2,3], Loïc Paulevé[1,2,4], Clair Poignard[5],
Mireille Régnier[1,2], Jean-Marc Steyaert[1,2], Laurent Schwartz[1,2,6]

[1] *LIX, École Polytechnique, Palaiseau, France*

[2] *INRIA-Saclay-île-de-France team AMIB, Palaiseau, France*

[3] *Cergy-Pontoise University, Cergy, France*

[4] *ETH Zürich, Switzerland*

[5] *INRIA Bordeaux Sud-Ouest, Bordeaux, France and*

[6] *Service d'oncologie, Hôpital Raymond Poincaré, Garches, France*

Abstract

Three physico-chemical cell parameters have been shown by the biologists to be of importance for understanding the cell behavior: the transmembrane potential (TMP) which modifies substantially the cell functional activity, the intracellular pH_i whose dynamics influences a number of other ionic fluxes and, to a lesser extent, the cell volume. In this work we present a dynamical model for understanding how the pH_i influences the TMP. In this model we consider the HCO_3^-/Cl^- and Na^+/H^+ exchangers as well as the bicarbonate/carbon dioxide buffering mechanism and also the ions conductance dependence to the intracellular pH_i.

We show that the conductances of the ions are the most important factors that have an impact on the TMP evolution and that the intracellular pH_i controls the membrane ionic conductance. Therefore, our new dynamical model support the hypothesis that pH_i regulates the TMP dynamics due its influence on membrane ionic conductances.

I. INTRODUCTION

Most chemical reactions in our body are carried out by special proteins called enzymes. Moreover, the intracellular hydrogen ion concentration $[H^+]$ (often denoted by $pH_i = -log[H^+]$) is known to control these enzyme's activities, which happens to be optimal in a narrow range of H^+ concentration. Hence, understanding the hydrogen ions dynamics is a key for understanding the cell behavior. Two other physical cell parameters have been shown to be of importance by biologists: the cell volume whose too large fluctuations can endanger cell survival [1] and the transmembrane potential (TMP) which modifies substantially the cell functional activity and affects its cell cycle [2–7].

Analysis of the experimental data [8–11] suggests that the intracellular pH_i and the transmembrane potential are strongly correlated.
The purpose of the current work is to explicit this relationship by means of a dynamical model, which describes the phenomena. We then proceed to simulations in order to give a precise mathematical understanding of the relationship.

Related work The relationship between the TMP and the ion fluxes has been addressed in several articles. In their seminal paper [3], Hodgkin and Huxley initiated the quantitative study of ion fluxes through the membranes applied to the conduction and excitation of nerve cells. In [2], Endresen *et al.* derive equations for the ionic currents that flow through channels, exchangers and electrogenic pumps. They establish the overall energy conservation of the cell and illustrate their theory in a model of spontaneously active cells in the cardiac pacemaker. More recently Clair *et al.* [12] have generalized the previous studies: their model links transmembrane potential, ionic concentrations and cell volume; they show that volume stabilization occurs within minutes of changes in extracellular osmotic pressure and infer a relationship between transmembrane potential and cell volume.

Contribution Our model is a generalization of the model described in [12], although we do not take into consideration the cell volume. It includes the HCO_3^-/Cl^- and Na^+/H^+ exchangers, the bicarbonate/carbon dioxide buffering mechanism and the pH_i dependence of the ion permeabilities — a new concept motivated from various experimental studies [9, 13, 14]. As is now familiar, the mathematical model is given by a set of ordinary differential equations (ODEs). Numerical simulations show that the conductances of the ions are the most important factors that have an impact on the TMP evolution. As it is described in [9],

the intracellular pH_i controls the membrane ionic conductance and therefore we formulate the following hypothesis: intracellular pH_i controls the TMP dynamics due to its influence on the membrane ionic conductances.

II. THE DYNAMICAL MODEL

In order to obtain a simple model of the pH influence on TMP through the permeabilities of ions, we consider hereafter that the outer concentrations of species is maintained constant - we assume here they are controlled by the external environment of the cell; and that the cell volume is constant.

A. Ion Fluxes and Transmembrane Potential

The transmembrane potential (TMP) sums up the electrical potentials due to the cell membrane and is driven by the ionic currents across the membrane. We use standard equations to derive TMP and ion fluxes evolutions [2, 3, 12] .

Given a ionic species S with valency (sum of charges) z_S, its equilibrium potential E_S can be obtained using the Nernst equilibrium equation:

$$E_S = \frac{R.T}{F.z_S} \log(\frac{[S]_{\mathrm{o}}}{[S]_{\mathrm{i}}}) \tag{1}$$

where R is the universal gas constant, F the Faraday constant, and T is temperature in Kelvin (fixed to 310K in the remaining of this paper). $[S]_{\mathrm{i}}$ (resp. $[S]_{\mathrm{o}}$) denotes the inner (resp.) outer concentration of species S.

The resting TMP, denoted by E_m, can then be expressed as the weighted sum of equilibrium potential of ions $\mathcal{I}$, weights being their respective permeability through the membrane.

$$E_m = \frac{\sum_{S\in\mathcal{I}} P_S.E_S}{\sum_{S\in\mathcal{I}} P_S} \tag{2}$$

where P_S is the membrane permeability for ion species S. In our model $\mathcal{I} = \{K^+, Na^+, Cl^-\}$.

Given a TMP value V_m, the ionic current I_S for S is then determined by first deriving its conductance g_S through the membrane (Eq. (3)), and is proportional to the difference between V_m and the equilibrium potential of S (Eq. (4)). The evolution of the TMP is

obtained with the Kirchoff law (Eq. (5)).

$$g_S = P_S.z_S^2.\frac{F^2}{2.R.T}.\sqrt{[S]_\mathrm{o}.[S]_\mathrm{i}} \tag{3}$$

$$I_S = g_S(V_m - E_S) \tag{4}$$

$$\frac{dV_m}{dt} = \frac{-\sum_{S\in\mathcal{I}} I_S}{C_m} \tag{5}$$

where C_m stands for the membrane conductance (fixed at 0.07 F.m^2).

Finally, the evolution of the inner concentration of species S due to its current follows the following equation:

$$\frac{d[S]_\mathrm{i}^\mathrm{Flux}}{dt} = -I_S\frac{\mathcal{A}}{z_S.F.\mathcal{V}} \tag{6}$$

where $\mathcal{A}$ and $\mathcal{V}$ are respectively the surface area and the volume of the cell. In the rest of this paper, the volume is assumed constant and the ratio $\mathcal{A}/\mathcal{V}$ has been fixed to $3/r$, with $r = 10^{-5}m$ being the radius of the cell (assumed spheric).

B. pH-Dependent Permeabilities

The existence of a pH-dependence for ions permeabilities has been hypothesized in several experimental studies [9, 13, 14]. The proposed equation is inspired from [9], where it has been successfully fitted to experimental data.

In the scope of this article, we focus on having only Na^+ permeability being pH-dependent, hence time-dependent, with $[H]_\mathrm{i}^t$ being the H^+ concentration at time t:

$$P_{Na^+}(t) = P_{Na^+}\frac{10^{-S_P.pK_{Na^+}}}{10^{-pK_{Na^+}.S_P} + [H]_\mathrm{i}^{tS_P}} \tag{7}$$

where pK_{Na^+} is the midpoint of pH-dependence, that is $P_{Na^+}(t) = \frac{P_{Na^+}}{2}$ when $[H]_\mathrm{i}^t = 10^{-pK_{Na^+}}$. S_P is the stiffness of this pH-dependence. Fig. 1 depicts the evolution of $P_{Na^+}(t)/P_{Na^+}$ with different parameters. In such a setting, P_{Na^+} should be considered as the maximum Na^+ permeability.

The above equation can be straightforwardly generalised for introducing pH-dependence for each ion permeabilities.

As it is discussed in Subsect. III B, the result on TMP regulation by pH relies on the varying ratios between ions permeabilities, where the effect is modulated by inner and outer ionic concentrations. In the scope of this article, we selected parameters such that a varying

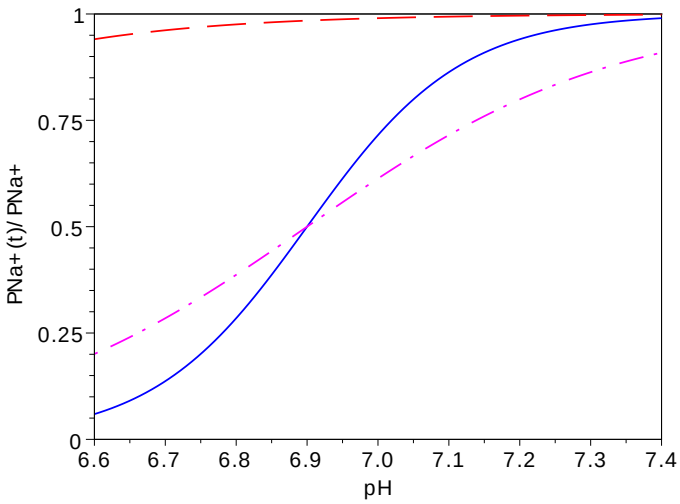

Figure 1: Proportion of the maximal permeability P_{Na^+} in function of pH. (plain curve) $pK_{Na^+} = 6.9$, $S_P = 4$; (dash-dotted curve) $pK_{Na^+} = 6.9$, $S_P = 2$; (dotted curve) $pK_{Na^+} = 6$, $S_P = 2$.

Na^+ permeability has the greatest impact on the TMP. With other concentrations and permeabilities settings our model should provide different conclusions.

C. pH Regulation Mechanisms

The regulation of pH within the cell is a very complex machinery involving numerous various biological processes. We consider here three important mechanisms: the bicarbonate buffer, and electro-neutrals Na^+/H^+ and HCO_3^-/Cl^- ionic exchangers.

a. Carbon dioxide/bicarbonate buffer Although CO_2 does not contain hydrogen ions it rapidly reacts with water to form carbonic acid H_2CO_3, which further dissociates into hydrogen and bicarbonate ions HCO_3^-. For the sake of simply, we retain a single reversible reaction:

$$CO_2 + H_2O \underset{k_2}{\overset{k_1}{\rightleftharpoons}} HCO_3^- + H^+ \tag{8}$$

where the ratio k_2/k_1 is the acid dissociation constant $pK_a = 6.37$. The water has to be considered as as abundant as needed.

Hence, this reversible reaction acts as a H^+ buffering mechanism, leading to a fixed balance between CO_2 and $HCO_3^- \cdot H^+$ concentrations. The impact of this buffering on species

concentrations evolution can be expressed as follows.

$$\frac{d[HCO_3]_{\mathrm{i}}^{\mathrm{Buf}}}{dt} = \frac{d[H^+]_{\mathrm{i}}^{\mathrm{Buf}}}{dt} = -\frac{d[CO_2]_{\mathrm{i}}^{\mathrm{Buf}}}{dt} = -k_1[HCO_3^-]_{\mathrm{i}}[H^+]_{\mathrm{i}} + k_2[CO_2]_{\mathrm{i}} \tag{9}$$

b. Na^+/H^+ unidirectional exchanger The role of Na^+/H^+ exchanger for limiting the cell inner acidity has been underlined by several experimental studies [15–19]

Basically, the exchanger is fully active when $[H^+]_{\mathrm{i}}$ is above a certain threshold $[H^+]^*$. In addition, this exchanger can be stopped when the cell obtain a too large volume. As we consider a constant cell size in our model, we ignored this latest feature, and propose the following equation for H^+ evolution concentration, assuming external concentrations constant:

$$\frac{d[Na^+]_{\mathrm{i}}^{\mathrm{nhe}}}{dt} = -\frac{d[H^+]_{\mathrm{i}}^{\mathrm{nhe}}}{dt} = k_{NHE}\frac{1+\tanh(\alpha([H^+]_{\mathrm{i}} - [H^+]^*) + \tanh^{-1}(1-\epsilon))}{2} \tag{10}$$

where k_{NHE} is the maximum rate of the exchanger and tanh the hyperbolic tangent. This term will tend toward k_{NHE} when $[H^+]_{\mathrm{i}} \gg [H^+]^*$, and tend toward zero when $[H^+]_{\mathrm{i}} \leq [H^+]$. α is a rescaling factor for the H^+ concentration difference, and has been set to 10^{10} in our simulations.

c. HCO_3^-/Cl^- bidirectional exchanger Due to the bicarbonate buffering, inner pH can also be controlled by varying HCO_3^- concentration. According to [18, 19], the HCO_3^-/Clm exchanger also play a role in pH regulation by acting on HCO_3^- inner concentration in order to maintain the pH around a certain threshold. For the sake of simplicity, we set this H^+ threshold identical to Na^+/H^+ mechanism (while it appears to be lower in practice [19]).

Assuming external concentrations constant, the activity of this exchanger is limited by inner HCO_3^- and Cl^- inner concentrations, and its direction depends on the sign $[H^+]_{\mathrm{i}} - [H^+]^*$. When $[H^+]_{\mathrm{i}}$ is above (resp. below) the threshold, the exchanger makes enter (resp. exit) HCO_3^- against Cl^-. This can be summarized by the following equation:

$$\frac{d[HCO_3^-]_{\mathrm{i}}^{\mathrm{ae}}}{dt} = -\frac{d[Cl^-]_{\mathrm{i}}^{\mathrm{ae}}}{dt} = k_{AE}.\tanh(\alpha([H^+]_{\mathrm{i}} - [H^+]^*))\frac{[HCO_3^-]_{\mathrm{i}}}{\beta_1 + [HCO_3^-]_{\mathrm{i}}}\frac{[Cl^-]_{\mathrm{i}}}{\beta_2 + [Cl^-]_{\mathrm{i}}} \tag{11}$$

where k_{AE} is the maximum rate of the exchanger, and β_1 and β_2 the respective saturation constants for HCO_3^- and Cl^- (set resp. to 0.001 and 0.03).

D. Full Model

In addition of the dynamics described above, we also consider a (constant) metabolic production of H^+ and CO_2. The full model can then be summarized as follows, where Na^+

permeability is computed using Eq. (7).

$$\frac{d[H^+]_\mathrm{i}}{dt} = H_{prod} + \frac{d[H^+]_\mathrm{i}^\mathrm{Buf}}{dt} - \frac{d[H^+]_\mathrm{i}^\mathrm{nhe}}{dt} \qquad \frac{d[CO_2]_\mathrm{i}}{dt} = CO_{2prod} - \frac{d[CO_2]_\mathrm{i}^\mathrm{Buf}}{dt}$$

$$\frac{d[Na^+]_\mathrm{i}}{dt} = \frac{d[NA^+]_\mathrm{i}^\mathrm{Flux}}{dt} + \frac{d[NA^+]_\mathrm{i}^\mathrm{nhe}}{dt} \qquad \frac{d[Cl^-]_\mathrm{i}}{dt} = \frac{d[Cl^-]_\mathrm{i}^\mathrm{Flux}}{dt} - \frac{d[Cl^-]_\mathrm{i}^\mathrm{ae}}{dt}$$

$$\frac{d[K^+]_\mathrm{i}}{dt} = \frac{d[K^+]_\mathrm{i}^\mathrm{Flux}}{dt} \qquad \frac{d[HCO_3^-]_\mathrm{i}}{dt} = \frac{d[HCO_3^-]_\mathrm{i}^\mathrm{Buf}}{dt} + \frac{d[HCO_3^-]_\mathrm{i}^\mathrm{ae}}{dt}$$

$$\frac{dV_m}{dt} = \frac{-\sum_{S\in\mathcal{I}} I_S}{C_m}$$

III. RESULTS

We first show simulation results supporting the pH influence on the dynamics of TMP for particular permeabilities of K^+, Na^+ and Cl^-, and having permeability of Na^+ being pH-dependent. Then, the sensitivity of this influence with respect to permeabilities parameters is studied in Subsect. III B. In particular, the simulations strongly suggest that the Na^+ pH-dependence plays a crucial role, and that the ratio of actual Na^+ permeability against K^+ permeability has to be above a certain threshold.

The selected parameters for our model are listed in Table I. Concentrations and permeabilities have been chosen to be within classical ranges [12, 19, 20]. For the purpose of our study, we enforce the pH to increase from 6.8 to 7.2 (i.e. $[H^+]_\mathrm{i}$ is divided by ≈ 2.5); which corresponds to some observed pH variation amplitudes during cell cycles [4, 5].

Simulations have been performed using the stiff ODE integrator shipped with Scilab [21].

A. pH influences the dynamics of TMP

In order to appreciate the effect of the pH-dependence of ions permeabilities on TMP dynamics, we first did some experiments without this pH-dependence enabled.

Fig. 2 shows the integration of our model including the ion fluxes and TMP equations (Subsect. II A) for the dashed curve; plus the pH regulation mechanisms (Subsect. II C) for the dash-dotted curve. In both cases, the permeability of Na^+ has been fixed to $\approx 0.28.P_{Na^+}$, which corresponds to its pH-dependent value when pH is 6.8 (Subsect. II B).

We observe that the regulation of pH has no impact on TMP dynamics. Indeed, despite the activation of Na^+/H^+ and HCO_3^-/Cl^- exchangers, the concentration of H^+ being very

Parameter	**Value**	**Description**	**Parameter**	**Value**	**Description**
P_{K^+}	4.10^{-8}	K^+ max. permeability	P_{Cl^-}	$1.2.10^{-7}$	Cl^- max. permeability
P_{Na^+}	$1.6.10^{-9}$	Na^+ max. permeability			
pK_{Na^+}	6.9	pH-dependence midpoint	S_P	4	pH-dependence stiffness
H_{prod}	10^{-9}	H^+ metabolic production	CO_{2prod}	2.10^{-10}	CO_2 metabolic production
k_{NHE}	$3.9.10^{-9}$	Na^+/H^+ exchanger rate	k_{AE}	$2.4.10^{-5}$	HCO_3^-/Cl^- exchanger rate
$[HCO_3^-]_i$	0.024	Inner HCO_3^- concentration	$[CO_2]_i$	0.0089	Inner CO_2 concentration
$[Na^+]_i$	0.0112	Inner Na^+ concentration	$[Na^+]_o$	0.145	Out. Na^+ concentration
$[K^+]_i$	0.139	Inner K^+ concentration	$[K^+]_o$	0.004	Out. K^+ concentration
$[Cl^-]_i$	0.0034	Inner Cl^- concentration	$[Cl^-]_o$	0.116	Out. Cl^- concentration
$[H^+]_i$	$10^{-6.8}$	Inner H^+ concentration	$[H^+]^*$	$10^{-7.2}$	Target $[H^+]_i$

Table I: Model parameters selected for Sect. III.

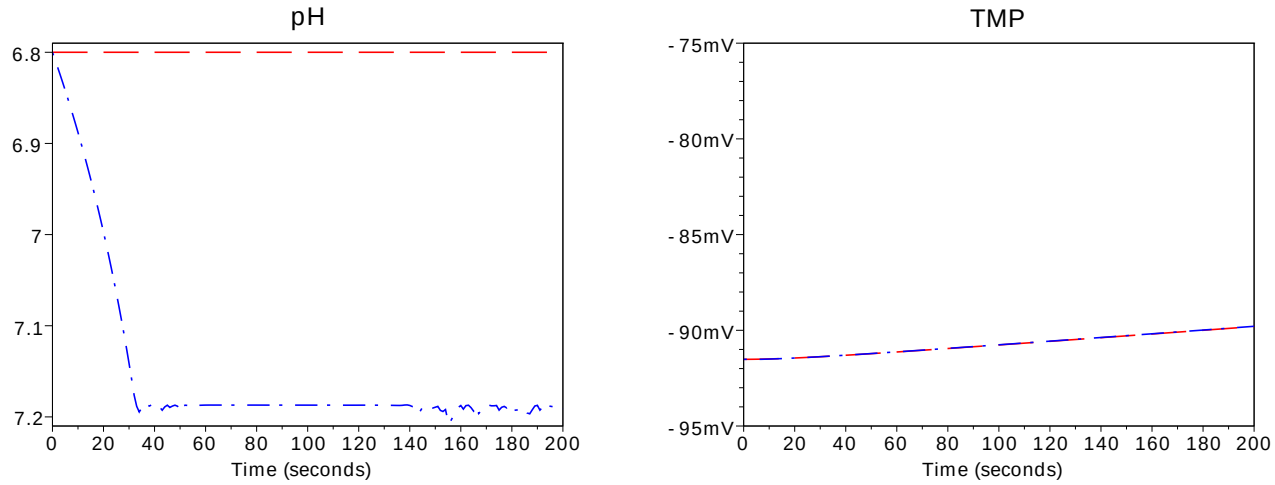

Figure 2: pH (left) and TMP (right) dynamics with only TMP equations (dashed curve) and with TMP together with pH regulation mechnisms (dash-dotted curve).

small in front of Na^+ and Cl^-, the variation induced in Na^+ and Cl^- concentrations is actually negligible. Thus, the sole regulation of pH should not impact the TMP.

We also remark that the TMP is not stable in our model settings. This is expected regarding the resting potential of K^+ and Na^+ ions ($E_{K^+} \approx -95$mV and $E_{Na^+} \approx +68$mV) their gradients make them inherently decrease and increase, respectively. As discussed in Sect. IV, future work may develop a more complete model, including notably the Na^+/K^+.

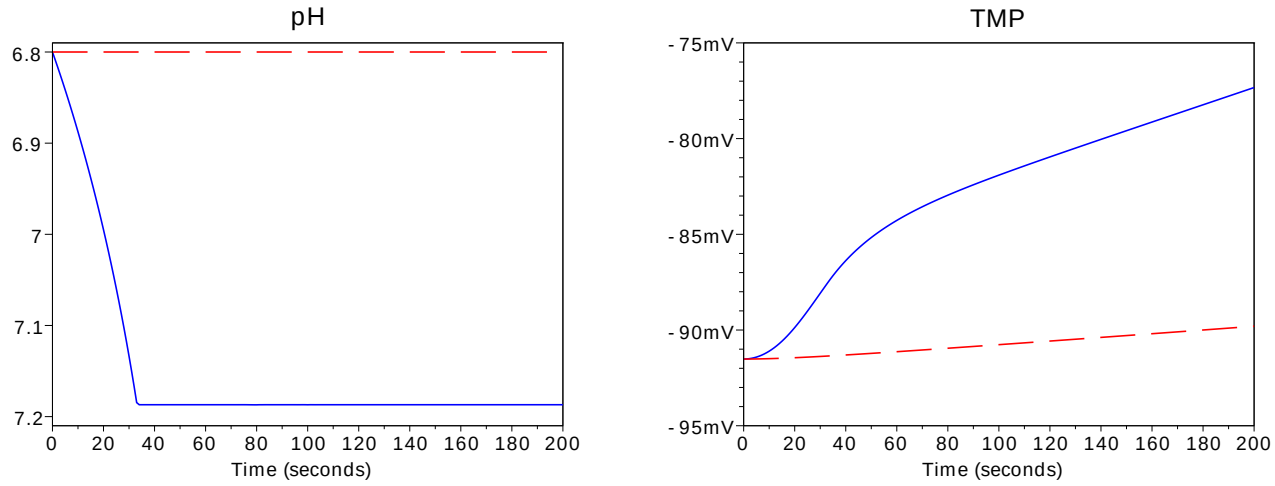

Figure 3: pH (left) and TMP (right) dynamics with only TMP equations (dashed curve) and with the full proposed model (plain curve).

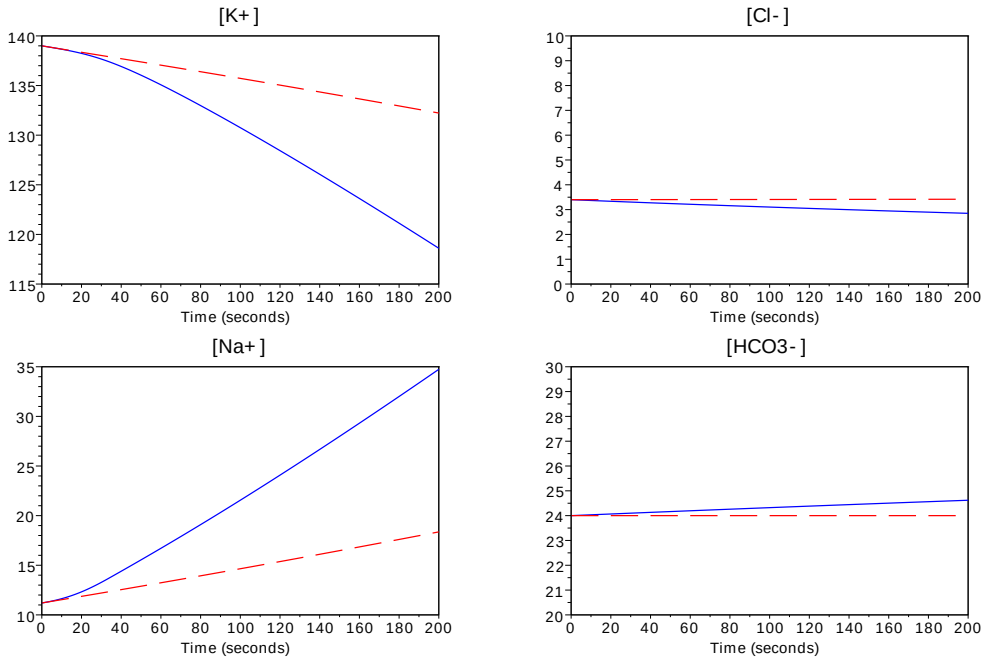

Figure 4: Inner concentration evolution (expressed in mmol) of K^+, Cl^-, Na^+, and HCO_3^-.

The integration of our complete model compared to the sub-model having only TMP equations is presented in Fig. 3 and Fig. 4.

The pH-dependence of Na^+ permeability makes it to modify the TMP significantly when pH varies. In the first 40 seconds, while pH moves from 6.8 to 7.2, the permeability of Na^+ goes from $\approx 0.28.P_{Na^+}$ to $\approx 0.94.P_{Na^+}$. Hence, Na^+ current is strongly increased, impacting

the global TMP. After 40 seconds, pH is stabilized, Na^+ permeability becomes constant and remain at a high value compared to the initial one, inducing a greater constant TMP decrease.

Fig. 4 details the concentration evolution of K^+, Cl^-, Na^+, and HCO_3^- in same setup as in Fig. 3. As previously discussed, the large variation of K^+ and Na^+ dynamics should not be attributed to the activation of Na^+/H^+ exchanger, but to the evolution of TMP (for K^+) and permeabilities (for Na^+). The tiny variation of Cl^- and HCO_3^- dynamics is mainly due to H^+ regulation by Cl^-/HCO_3^- exchanger.

B. Parameters sensitivity

As recalled in Subsect. II A, at constant temperature, while the equilibrium potential of ions is solely determined by the ratio of their inner and outer concentration, the resting TMP follows a weighted sum of those equilibrium potential, the weights being the ions permeabilities through the membrane. The flux of each ion is then proportional to the difference between its proper equilibrium potential and the global TMP, and proportional to its permeability.

In such a setting, the TMP is controlled by both ions inner and outer concentrations and their permeabilities. Focusing on permeabilities, the *crucial factor* is their mutual ratios (because of the weighted sum). Hence, the pH influence on TMP is explained by the ratio between Na^+ and both K^+ and Cl^- permeabilities which significantly varies alongside the H^+ concentration.

Given the selected initial ions concentrations (Table I), the resting TMP is around -91mV, and the ions resting potential are $E_{K^+} \approx -95\text{mV}$, $E_{Na^+} \approx +68\text{mV}$ and $E_{Cl^-} \approx -94\text{mV}$. Hence, we notice that E_{K^+} and E_{Cl^-} are actually close to initial TMP, resulting in low ionic currents through the membrane. On the contrary, E_{Na^+} present an opposite value, indicating a high current, however restrained by the (typically) low Na^+ permeability. But, because E_{Na^+} is so different from E_{K^+} and E_{Cl^-}, even with a low permeability with respect to K^+, a variation in Na^+ permeability should have impact a noticeable impact on the TMP.

This is notably illustrated in Fig. 5 by integrating TMP dynamics with different permeability ratios settings (left figure), or with different pH-dependence for Na^+ permeabilities. The other parameters are identical as in previous section, and the full model is considered.

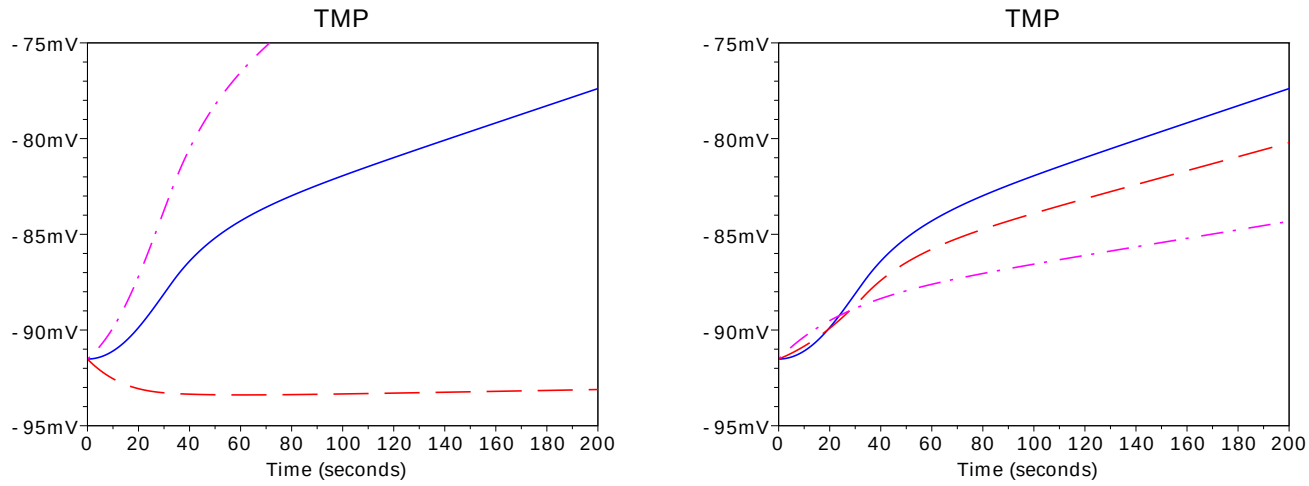

Figure 5: (left) Integrated TMP with $P_{Na^+} = 0.004$ (dashed), 0.04 (plain), 0.07 (dash-dotted); (right) Integrated TMP with $S_P = 0.1$ (dash-dotted), 2 (dashed), 4 (plain).

In Fig. 5(left), the maximal permeability P_{Na^+} ranges through $0.004P_{K^+}$, $0.04P_{K^+}$ (default value), and $0.07P_{K^+}$, showing the strong impact of the P_{Na^+}/P_{K^+} ratio. We notice that a too small ratio (below 1%) makes E_{Na^+} negligible for TMP.

In Fig. 5(right), the stiffness of the pH-dependence for P_{Na^+} is controlled by tuning the S_P parameter. With a low S_P parameter, the Na^+ slowly varies with respect to pH, while a high S_P induces a large variance. As predicted, the higher S_P, the stronger TMP regulation.

IV. DISCUSSION

We presented a new dynamical model of ions fluxes through the cell membrane which emphasizes the regulation of the cell transmembrane potential (TMP) by the varying intracellular pH and ions permeabilities.

As stated in the introduction and in Subsect. II B, various experimental studies already support the hyothesis that inner pH controls ions permeabilities, and thus affect the cell TMP. Our model brings a mathematical analysis of this possibly involved regulation mechanism, and calls for further experimental validations.

Future work will incorporate additional ions regulation mechanisms, such as the Na^+/K^+ pumps [22], and will consider a dynamical cell volume with osmolarity pressure (as it has been done in prior work in [12]). Finally, the modelling of the impact of pH on

cell mitosis is under investigation.

---

[1] F. Lang, G. L. Busch, M. Ritter, H. Vlkl, S. Waldegger, E. Gulbins, and D. Hussinger, Physiol Rev **78**, 247 (1998).

[2] L. Endresen, H. J. K. Hall, and J. Myrheim, Eur. Biophys. J. **29**, 90 (2000).

[3] A. L. Hodgkin and A. F. Huxley, J. Physiol. **117**, 500 (1952).

[4] W. B. Busa and R. Nuccitelli, The American journal of physiology **246**, R409 (1984), ISSN 0002-9513.

[5] R. J. Aerts, A. J. Durston, and W. H. Moolenaar, Cell **43**, 653 (1985), ISSN 0092-8674.

[6] D. J. Blackiston, K. A. McLaughlin, and M. Levin, Cell cycle (Georgetown, Tex.) **8**, 3519 (2009), ISSN 1551-4005.

[7] S. Sundelacruz, M. Levin, and D. Kaplan, Stem Cell Reviews and Reports **5**, 231 (2009), ISSN 1550-8943, 10.1007/s12015-009-9080-2.

[8] C. E. Bear, J. S. Davison, and E. A. Shaffer, Biochimica et Biophysica Acta (BBA) - Biomembranes **944**, 113 (1988), ISSN 0005-2736.

[9] B. J. Harvey, S. R. Thomas, and J. Ehrenfeld, J. Gen. Physiol. **92**, 767 (1988).

[10] J. G. Fitz, T. E. Trouillot, and B. F. Scharschmidt, The American journal of physiology **257**, G961 (1989), ISSN 0002-9513.

[11] J. A. Fraser, C. E. Middlebrook, J. A. Usher-Smith, C. J. Schwiening, and C. L.-H. Huang, The Journal of Physiology **563**, 745 (2005), ISSN 1469-7793.

[12] C. Poignard, A. Silve, F. Campion, L. Mir, M., O. Saut, and L. Schwartz, European Biophysics Journal: EBJ **40** (2011), aRC C3MB.

[13] H. M. Brown, S. Hagiwara, H. Koike, and R. M. Meech, The Journal of Physiology **208**, 385 (1970), http://jp.physoc.org/content/208/2/385.full.pdf+html.

[14] H. Oberleithner, U. Kersting, and M. Hunter, Proceedings of the National Academy of Sciences **85**, 8345 (1988).

[15] J. Lacroix and et al., EMBO reports pp. 91–96 (2004).

[16] R. A. Cardone, V. Casavola, and S. J. Reshkin, Nat Rev Cancer **5**, 786 (2005).

[17] C. M. Armstrong, P.N.A.S **100**, 6257 (2003).

[18] C. C. Aickin and R. C. Thomas, The Journal of physiology **273**, 295 (1977), ISSN 0022-3751.

[19] R. A. Cardone, V. Casavola, and S. J. Reshkin, Nat Rev Cancer **5**, 786 (2005).

[20] N. K. Martin, E. A. Gaffney, R. A. Gatenby, R. J. Gillies, I. F. Robey, and P. K. Maini, Math Biosci **230**, 1 (2011).

[21] Scilab Enterprises, *Scilab: free open source software for numerical computing*, Orsay, France (2012), URL `http://www.scilab.org`.

[22] C. M. Armstrong, Proceedings of the National Academy of Sciences **100**, 6257 (2003), http://www.pnas.org/content/100/10/6257.full.pdf+html.